Am J Transl Res 2017;9(8):3827-3841
www.ajtr.org /ISSN:1943-8141/AJTR0055089

Original Article

Therapeutic effect of rosuvastatin and propylthiouracil on ameliorating high-cholesterol diet-induced fatty liver disease, fibrosis and inflammation in rabbit

Pao-Yuan Lin[1*], Chih-Hung Chen[2*], Christopher Glenn Wallace[10], Kuan-Hung Chen[3], Chia-Lo Chang[4], Hong-Hwa Chen[4], Pei-Hsun Sung[5], Kun-Chen Lin[3], Sheung-Fat Ko[6], Cheuk-Kwan Sun[11], Hsueh-Wen Chang[12], Pei-Lin Shao[13], Mel S Lee[7], Hon-Kan Yip[5,8,9,13,14]

[1]Department of Plastic and Reconstructive Surgery, [2]Divisions of General Medicine, Department of Internal Medicine, [3]Department of Anesthesiology, [4]Division of Colorectal Surgery, Department of Surgery, [5]Division of Cardiology, Department of Internal Medicine, [6]Department of Radiology, [7]Department of Orthopedics, [8]Institute for Translational Research in Biomedicine, [9]Centers for Shockwave Medicine and Tissue Engineering, Kaohsiung Chang Gung Memorial Hospital, College of Medicine, Chang Gung University, Kaohsiung 83301, Taiwan; [10]Department of Plastic Surgery, University Hospital of South Manchester, Manchester, UK; [11]Department of Emergency Medicine, E-DA Hospital, I-Shou University, Kaohsiung 82445, Taiwan; [12]Department of Biological Sciences, National Sun Yat-sen University, Kaohsiung 80424, Taiwan; [13]Department of Nursing, Asia University, Taichung 41354, Taiwan; [14]Department of Medical Research, China Medical University Hospital, China Medical University, Taichung 40402, Taiwan. [*]Equal contribution.

Received April 10, 2017; Accepted July 16, 2017; Epub August 15, 2017; Published August 30, 2017

Abstract: This study tested the hypothesis that high-cholesterol diet (HCD)-induced fatty liver disease could be ameliorated by rosuvastatin (Ros) and propylthiouracil (PTU) therapy. Thirty-two Zealand rabbits were equally divided into group 1 (sham-control), group 2 (HCD for 8 weeks), group 3 [HCD-Ros (20 mg/kg/day administration after 4-week HFD for 4 weeks)], group 4 [HCD-PTU (0.1% PTU in drinking water) with treatment course as group 3]. Liver weight, fibrosis, collagen deposition area, and serum levels of AST/ALT were highest in group 2, lowest in group 1, and significantly higher in group 4 than group 3 (all P<0.0001). The levels of inflammatory (TNF-α/NF-κB/IL-1ß/IL-6/MMP-9/VCAM-1/PAI-1/TLR-4, MyD88/IL-12/IFN-γ), oxidative stress (NOX-1/NOX-2/oxidized protein), apoptotic (Bax/cleaved-capase-3/PARP), fibrotic (Smad-3/TGF-ß), and mitochondria-damaged (cytosolic-cytochrome-C) proteins showed an identical pattern, whereas antiapoptotic (Bcl-2), mitochondrial-integrity (mitochondrial-cytochrome-C) and antioxidative (SIRT1/SIRT3) biomarkers exhibited an opposite pattern to fibrosis among the four groups (all P<0.0001). The cellular expressions of inflammatory (Kupffer/CD14/CD44), α-fetoprotein-positively stained biomarkers, apoptotic nuclei and fat cells displayed an identical pattern to fibrosis (all P<0.0001). In conclusion, Ros-PTU therapy attenuated liver fibrosis, inflammatory reaction and generation of oxidative stress and fatty liver after HCD challenge in rabbits.

Keywords: Oxidative stress, inflammation, hypercholesterolemia, liver fibrosis, fatty liver

Introduction

Metabolic syndrome (MetS) is increasingly common worldwide, reflecting rising obesity rates in children and adults, and may overtake smoking as the leading risk factor for coronary artery disease (CAD) [1-3]. MetS is also is an independent risk factor for the development of nonalcoholic fatty liver disease (NAFLD), suggesting that NAFLD may be a hepatic manifestation of MetS [1-7]. The prevalence of NAFLD is also increasing worldwide and is a common cause of chronic liver disease, which can progress to cirrhosis and liver failure [8-12]. Presentation ranges from simple steatosis to non-alcoholic steatohepatitis (NASH) [1-12]. NAFLD and NASH are the most common causal etiologies of chronic liver disease with well-known detriment to patients' health-related quality of life [9, 10]. It is clear that patients with NAFLD are at increased risk of cardiovascular events, which are the leading cause of death in this population [13]. Furthermore, there is mounting evidence that an increased risk of hepatocellular

carcinoma (HCC) exists in NAFLD patients, even outstripping other etiologies in some high-income countries [14-17]. Clinical observation studies have also established that the hepatic manifestation of MetS can predispose patients to HCC in the absence of cirrhosis or advanced fibrosis [16].

Although the link between MetS and NASH/NAFLD is well established and the impact of NASH/NAFLD on unfavorable clinical outcomes has been extensively investigated [14-18], the pathogenesis and mechanisms underlying MetS-caused NASH/NAFLD is not well understood [1]. Furthermore, an effective treatment for NASH/NAFLD is not yet available [12].

Statins have unique anti-inflammatory properties [18] that suppress the production of reactive oxygen species (ROS) [19, 20] and oxidant/free radicals [21, 22]. Statins inhibit plaque formation and attenuate plaque burden in human coronary arteries [23] and rabbit aortas [24]. We have previously demonstrated that propylthiouracil (PTU), a thiouracil-derivative used to treat hyperthyroidism, ameliorates monocrotaline-induced pulmonary artery hypertension in rodent, mainly through suppressing inflammation and enhancing nitric oxide (NO) production [25]. Accordingly, this study tested the hypothesis that statin and PTU therapy could attenuate high-cholesterol diet (HCD)-induced fatty liver disease and fibrosis of liver parenchyma, mainly through reducing inflammation and the generation of oxidative stress, as well as upregulating anti-oxidant and anti-oxidative stress signaling.

Materials and methods

Ethics

All animal experimental protocols and procedures were approved by the Institute of Animal Care and Use Committee at Kaohsiung Chang Gung Memorial Hospital (Affidavit of Approval of Animal Use Protocol No. 2014021801) and performed in accordance with the Guide for the Care and Use of Laboratory Animals [The Eighth Edition of the Guide for the Care and Use of Laboratory Animals (NRC 2011)].

Animals were housed in an Association for Assessment and Accreditation of Laboratory Animal Care International (AAALAC)-approved animal facility in our hospital (IACUC protocol no. 101008) with controlled temperature and light cycles (24°C and 12/12 light cycles).

Experimental protocol for high-fat diet (HCD)-induced nonalcoholic fatty liver disease (NAFLD)

The purpose of this experimental model of HCD-induced fatty liver was to mimic the clinical setting of hypercholesterolemia induced NAFLD. The procedure and protocol for HCD-induced fatty liver have recently been described [26]. In detail, thirty-two New Zealand white rabbits weighing 2.2 to 2.5 kg were purchased from BioLasco Technology (Taiwan). They were categorized into four diet groups: (1) Control diet (n=8); (2) 2% high-cholesterol diet [HCD only; n=8; purchased from Test Diet (Richmond, IN)]; (3) 2% HCD plus rosuvastatin administration (20 mg/kg/day; n=8); and (4) 2% HCD plus PTU (0.1% PTU in drinking water; n=8).

Rosuvastatin and PTU treatment began after 4 weeks of HCD feeding and was continued for 4 weeks. The rationale for this PTU therapy regimen was based on our previous report [25, 26]. Briefly, the 0.1% PTU in 100 ml water was equivalent to 0.27 mg per 100 ml of drinking water, which was the average daily water consumption for each animal in our study. The safety and efficacy of this therapy regimen were assessed in our previous work [25, 26]. Additionally, the therapy regimen of rosuvastatin was based on our previous report [26, 27]. After total 8 weeks of study, rabbits were sacrificed and livers were harvested for further analyses.

Biochemical examinations

Rabbit sera were analyzed for blood sugar level, thyroid function (free T4) and lipids, including total cholesterol (TC), high density lipoprotein cholesterol (HDL-C), low density lipoprotein cholesterol (LDL-C) and triglycerides [26] as well as serum level of serum levels of aspartate transaminase (AST) and alanine transaminase (ALT).

Western blot analysis

The procedure and protocol for Western blot analysis were based on our recent reports [28-30]. In detail, equal amounts (50 mg) of protein extracts were loaded and separated by SDS-PAGE using acrylamide gradients. After electrophoresis, the separated proteins were transferred electrophoretically to a polyvinylidene di-

fluoride (PVDF) membrane (GE, UK). Nonspecific sites were blocked by incubation of the membrane in blocking buffer [5% nonfat dry milk in T-TBS (TBS containing 0.05% Tween 20)] overnight. The membranes were incubated with the indicated primary antibodies [Caspase 3 (1:1000, Cell Signaling), Poly (ADP-ribose) polymerase (PARP) (1:1000, Cell Signaling), matrix metallo), tuproteinase (MMP)-9 (1:3000, Abcam), nuclear factor (NF)-κB (1:1000, Abcammor necrosis factor (TNF)-α (1:1000, Cell Signaling), interleukin (IL)-1b (1:1000, Cell Signaling), intercellular adhesion molecule (ICAM)-1 (1:1000, Abcam), plasminogen activator inhibitor (PAI-1) (1:1000, Abcam), toll-like receptor (TLR)-4 (1:500, Novus Biologicals), myeloid differentiation factor 88 (MyD88) (1:1000, Abcam), IL-6 (1:750, Abcam), IL-12 (1:500, Abcam) and interferon (IF)-γ (1:1000, Abcam), SIRT1 (1:4000, Abcam), SIRT3 (1:500, Abcam), Bax (1:1000, Abcam), cytosolic cytochrome (c-Cyt) C (1:1000, BD), mitochondrial cytochrome (m-Cyt) C (1:1000, BD), NOX-1 (1:1500, Sigma), NOX-2 (1:750, Sigma), γ-H2AX (1:1000, Cell Signaling), andactin (1:1000, Millipore)] for 1 hour at room temperature. Horseradish peroxidase-conjugated anti-rabbit immunoglobulin (IgG; 1:2000, Cell Signaling, Danvers, MA, USA) was used as a secondary antibody for one-hour incubation at room temperature. The washing procedure was repeated eight times within one hour. Immunoreactive bands were visualized by enhanced chemiluminescence (ECL; Amersham Biosciences, Amersham, UK) and exposed to Biomax L film (Kodak, Rochester, NY, USA). For quantification, ECL signals were digitized using Labwork software (UVP, Waltham, MA, USA).

Immunohistochemical (IHC) and immunofluorescent (IF) staining

The procedure and protocol for IF staining have been detailed in our previous reports [28-30]. For IHC and IF staining, rehydrated paraffin sections were first treated with 3% H_2O_2 for 30 minutes and incubated with Immuno-Block reagent (BioSB, Santa Barbara, CA, USA) for 30 minutes at room temperature. Sections were then incubated with primary antibodies specifically against r-H2AX (1:500, Abcam), Kupffer cell (Monoclonal Mouse Anti-Rabbit Macrophage, Clone RAM11, 1:400, Dako), α-fetoprotein (1:50, Abcam), CD44 (1:500, GeneTex), TUNLE assay (In Situ Cell Death Detection Kit, POD, Roche), and CD14 (1:50, Santa Cruz), while sections incubated with the use of irrelevant antibodies served as controls. Three sections of liver from each rabbit were analyzed. For quantification, three randomly selected high-power fields (HPFs) (200× or 400× for IHC and IF studies, respectively) were analyzed in each section. The mean number of positively-stained cells per HPF for each animal was then determined by summation of all numbers divided by 9.

Assessment of oxidative stress

The procedure and protocol for evaluating protein expression of oxidative stress have been detailed in our previous reports [28-30]. The Oxyblot Oxidized Protein Detection Kit was purchased from Chemicon, Billerica, MA, USA (S7150). DNPH derivatization was carried out on 6 μg of protein for 15 minutes according to the manufacturer's instructions. One-dimensional electrophoresis was carried out on 12% SDS/polyacrylamide gel after DNPH derivatization. Proteins were transferred to nitrocellulose membranes that were then incubated in the primary antibody solution (anti-DNP 1:150) for 2 hours, followed by incubation in secondary antibody solution (1:300) for 1 hour at room temperature. The washing procedure was repeated eight times within 40 minutes. Immunoreactive bands were visualized by enhanced chemiluminescence (ECL; Amersham Biosciences, Amersham, UK) which was then exposed to Biomax L film (Kodak, Rochester, NY, USA). For quantification, ECL signals were digitized using Labwork software (UVP, Waltham, MA, USA). For oxyblot protein analysis, a standard control was loaded on each gel.

Histological quantification of liver fibrosis and collagen deposition area

Masson's trichrome staining and Sirius red staining were used for assessing liver fibrosis and collagen deposition areas, respectively. Three serial sections of liver in each animal were prepared at 4 μm thickness by Cryostat (Leica CM3050S). The integrated area (μm^2) of fibrotic area and collagen deposition area on each section were calculated using the Image Tool 3 (IT3) image analysis software (University of Texas, Health Science Center, San Antonio, UTHSCSA; Image Tool for Windows, Version 3.0, USA). Three randomly selected high-power fields (HPFs) (100×) were analyzed in each section. After determining the number of pixels in each fibrotic and collagen deposition area per

Table 1. Biochemical parameters, thyroid function and body weight by the end of 8 weeks after HCD administration (n=8 for each group)

Variables	Control diet	HCD	HCD-Ros	HCD-PTU	*p*-value
Total cholesterol (mg/dL)	59 ± 15[a]	1855 ± 547[b]	760 ± 94[c]	923 ± 167[d]	<0.0001
LDL (mg/dL)	12 ± 3[a]	528 ± 144[b]	284 ± 43[c]	389 ± 34[d]	<0.0001
TG (mg/dL)	66 ± 29[a]	247 ± 54[b]	168 ± 24[c]	104 ± 24[d]	<0.001
Sugar (mg/dL)	161 ± 34	156 ± 40	147 ± 37	153 ± 26	0.642
Free T4 (ng/dL)	1.43 ± 0.29	1.42 ± 0.25	1.39 ± 0.33	1.30 ± 0.30	0.684
Body weight (kg)	3.48 ± 0.10	3.38 ± 0.21	3.24 ± 0.27	3.20 ± 0.25	0.426

Data are expressed as mean ± SD. HCD = high-cholesterol diet; TG = triglyceride; Ros = rosuvastatin; PTU = propylthiouracil. Symbols ([a, b, c, d]) indicate significance (at 0.05 level).

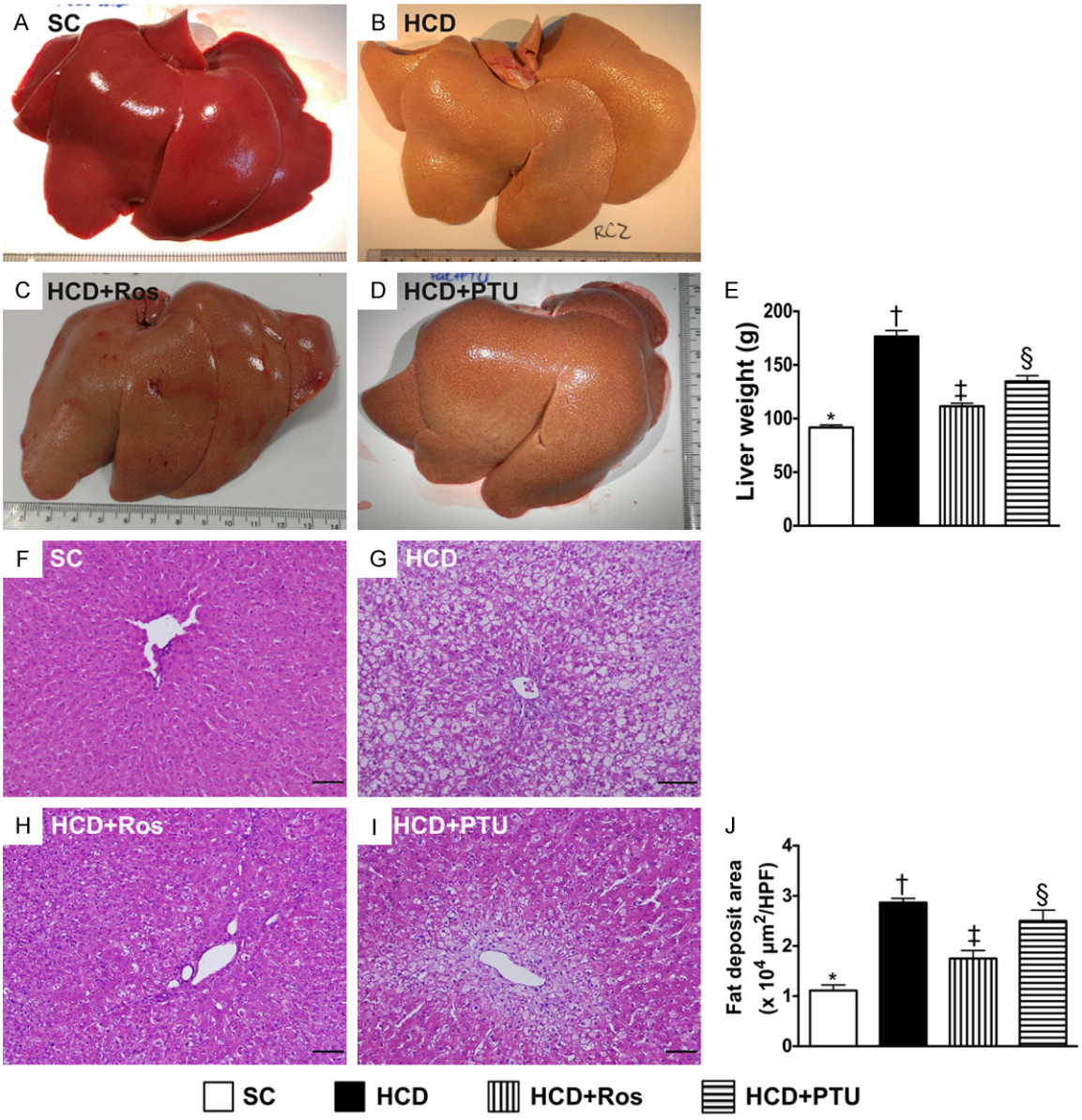

Figure 1. Liver morphology and weight and histopathological findings of liver parenchyma at the 8th week after HCD feeding. A-D: Illustrating the grossly anatomical feature of liver among the four groups. The remarkably fatty liver in HCD group than in other groups was clearly identified. E: Total liver weight, *vs. other groups with different symbols (†, ‡, §), P<0.001. F-I: Illustrating the H&E light microscopy (100×) for identification of inflamed fatty liver

(i.e. steatohepatitis with bright color). Note that the triglyceride droplet vacuoles in the tissue cells of the liver were clearly recognized. J: Analytical result of the fat-deposit area in liver, *vs. other groups with different symbols (†, ‡, §), P<0.0001. Scale bars in right lower corner represent 100 μm. All statistical analyses were performed by one-way ANOVA, followed by Bonferroni multiple comparison post hoc test (n=8 for each group). Symbols (*, †, ‡, §) indicate significance (at 0.05 level). SC = sham control; HCD = high-cholesterol diet; Ros = rosuvastatin; PTU = propylthiouracil. HPF = high-power field.

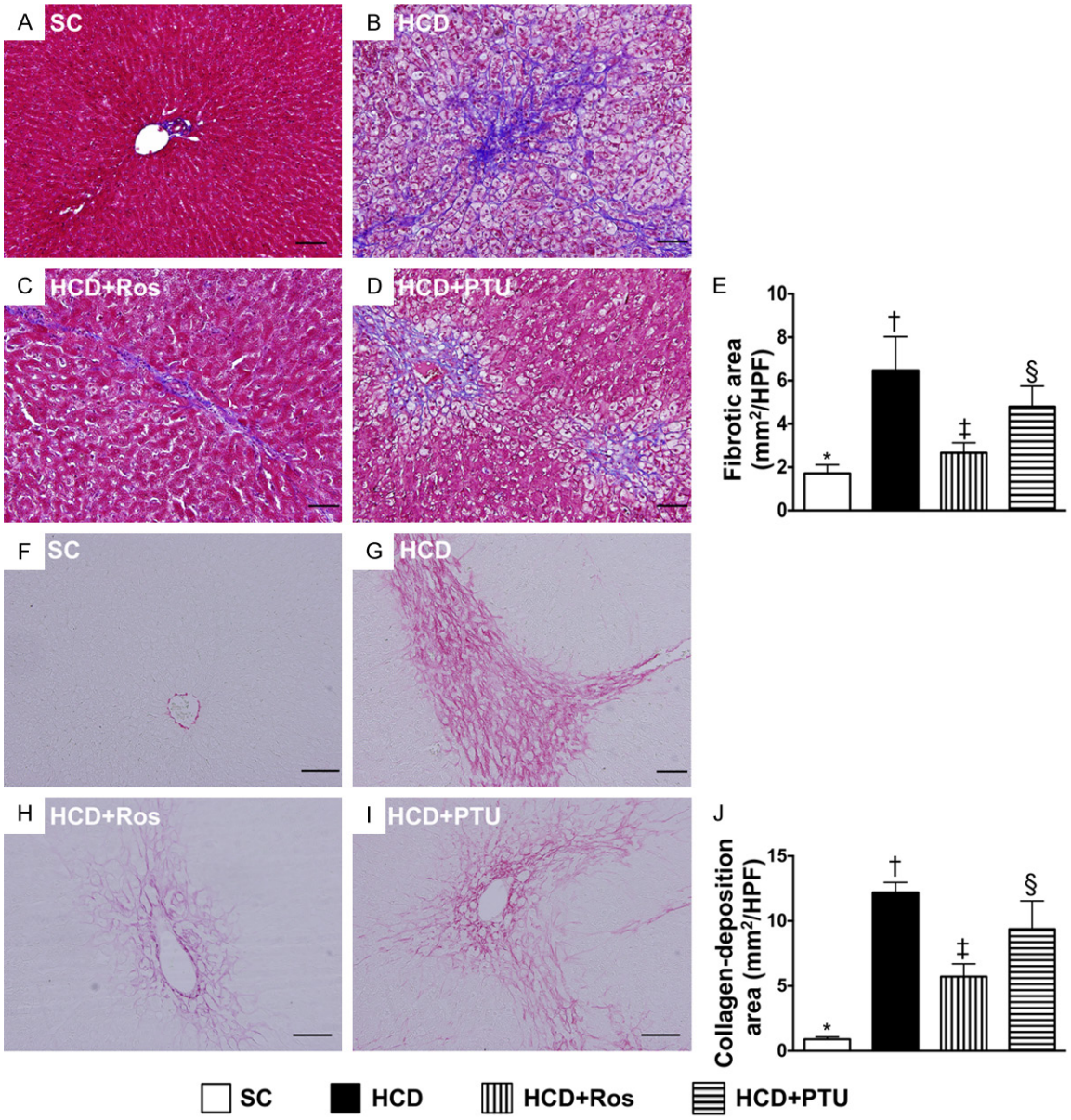

Figure 2. Fibrosis and collagen deposition areas in liver parenchyma at the 8th week after HCD feeding. A-D: Illustrating microscopic finding (100×) of Masson's trichrome staining for identification of fibrosis area (blue). E: Analytical result of fibrosis area, *vs. other groups with different symbols (†, ‡, §), P<0.0001. F-I: Illustrating microscopic finding (100×) of Sirius red staining for identification of collagen deposition area (pink). J: Analytical result of collagen deposition area, *vs. other groups with different symbols (†, ‡, §), P<0.0001. Scale bars in right lower corner represent 100 μm. All statistical analyses were performed by one-way ANOVA, followed by Bonferroni multiple comparison post hoc test (n=8 for each group). Symbols (*, †, ‡, §) indicate significance (at 0.05 level). SC = sham control; HCD = high-cholesterol diet; Ros = rosuvastatin; PTU = propylthiouracil. HPF = high-power field.

HPF, the numbers of pixels obtained from three HPFs were summated. The procedure was repeated in two other sections for each animal. The mean pixel number per HPF for each ani-

mal was then determined by summating all pixel numbers and dividing by 9. The mean integrated area (μm^2) of fibrosis and collagen deposition in liver per HPF was obtained using a conversion factor of 19.24 (1 μm^2 represented 19.24 pixels).

Statistical analyses

Quantitative data are expressed as means ± SD. Statistical analyses were performed by ANOVA, followed by Bonferroni multiple-comparison post hoc test. SAS statistical software for Windows version 8.2 (SAS institute, Cary, NC) was utilized. A *P* value of less than 0.05 was considered statistically significant.

Results

*Lipid profile and thyroid function 8 weeks after HCD administration (**Table 1**)*

The results in **Table 1**, which were adapted with permission from Lin PY, et al. [26], expressed the blood levels of total cholesterol, low-density lipoprotein (LDL), triglyceride (TG), blood sugar and free T4, as well as body weight at the end of study before sacrifice of animals. At the end of the study period (i.e. at the 8th week after HCD feeding), plasma levels of free T4 and sugar were not different among the four groups, suggesting that the 0.1% PTU in drinking water did not influence thyroid function of the rabbits. The final body weight also was similar among the four groups. However, the serum levels of total cholesterol, LDL and TG were highest in group 2 (i.e. CHD only), lowest in group 1 (i.e. control group), and significantly higher in group 4 (i.e. HCD + PTU) than in group 3 (i.e. HCD + rosuvastatin).

*Liver morphology and weight and histopathological findings of liver parenchyma at the 8th week after HCD feeding (**Figure 1**)*

The grossly anatomical feature showed that as compared with group 1, severe fatty liver was clearly identified in group 2 that was markedly reversed in groups 3 and 4. Additionally, liver weight was significantly higher in group 2 than in groups, 1, 3 and 4, significantly higher in group 4 than in groups 1 and 3, and significantly higher in group 1 than in group 3. Furthermore, H&E light microscopy showed that there was accumulation of triglyceride droplet vacuoles in the tissue cells of the liver in group 2 animals, suggesting that inflamed liver with fatty occurred in the animals. However, this situation was identified to be reversible in groups 3 and 4. Importantly, analytical results showed that the area of inflamed liver with fatty (i.e. steatohepatitis) exhibited an identical pattern to liver weight among the four groups.

*Fibrosis and collagen deposition areas at the 8th week after HCD feeding (**Figure 2**)*

Masson's trichrome staining showed that the fibrosis area in liver parenchyma was highest in group 2, lowest in group 1, and significantly higher in group 4 than in group 3. Additionally, Sirius red staining demonstrated that the collagen deposition area showed an identical pattern to fibrosis among the four groups.

*The protein expression of inflammatory biomarkers at the 8th week after HCD feeding (**Figure 3**)*

The protein expression of PAI-1, ICAM-1, IL-1ß, TNF-α, TLR-4, MyD88, IL-6, IL-12 and INF-γ, nine inflammatory biomarkers, were highest in group 2, lowest in group 1 and significantly higher in group 4 than in group 3.

*The protein expression of apoptotic, anti-apoptotic and oxidative stress biomarkers at the 8th week after HCD feeding (**Figure 4**)*

The protein expressions of cleaved caspase3, Bax and cleaved PARP, three indicators of apoptosis, were highest in group 2, lowest in group 1, and significantly higher in group 4 than group 3. Additionally, the protein expressions of NOX-1, NOX-2 and oxidized protein, three indices of oxidative stress, also showed an identical pattern to apoptosis among the four groups. Additionally, the protein level of γ-H2AX, a marker for DNA damage, exhibited an identical pattern to apoptotsis.

*The protein expressions of fibrotic, anti-fibrotic, mitochondrial damage, mitochondrial-integrity and anti-oxidative stress biomarkers at the 8th week after HCD feeding (**Figure 5**)*

The protein expression of phosphorylated (p)-Smad3 and TGF-ß, two indicators of fibrosis, were highest in group 2, lowest in group 1, and significantly higher in group 4 than in group 3. On the other hand, the protein expression of p-Smad1/5 and BMP-2, two indicators of anti-fibrosis, showed an opposite pattern to fibrosis.

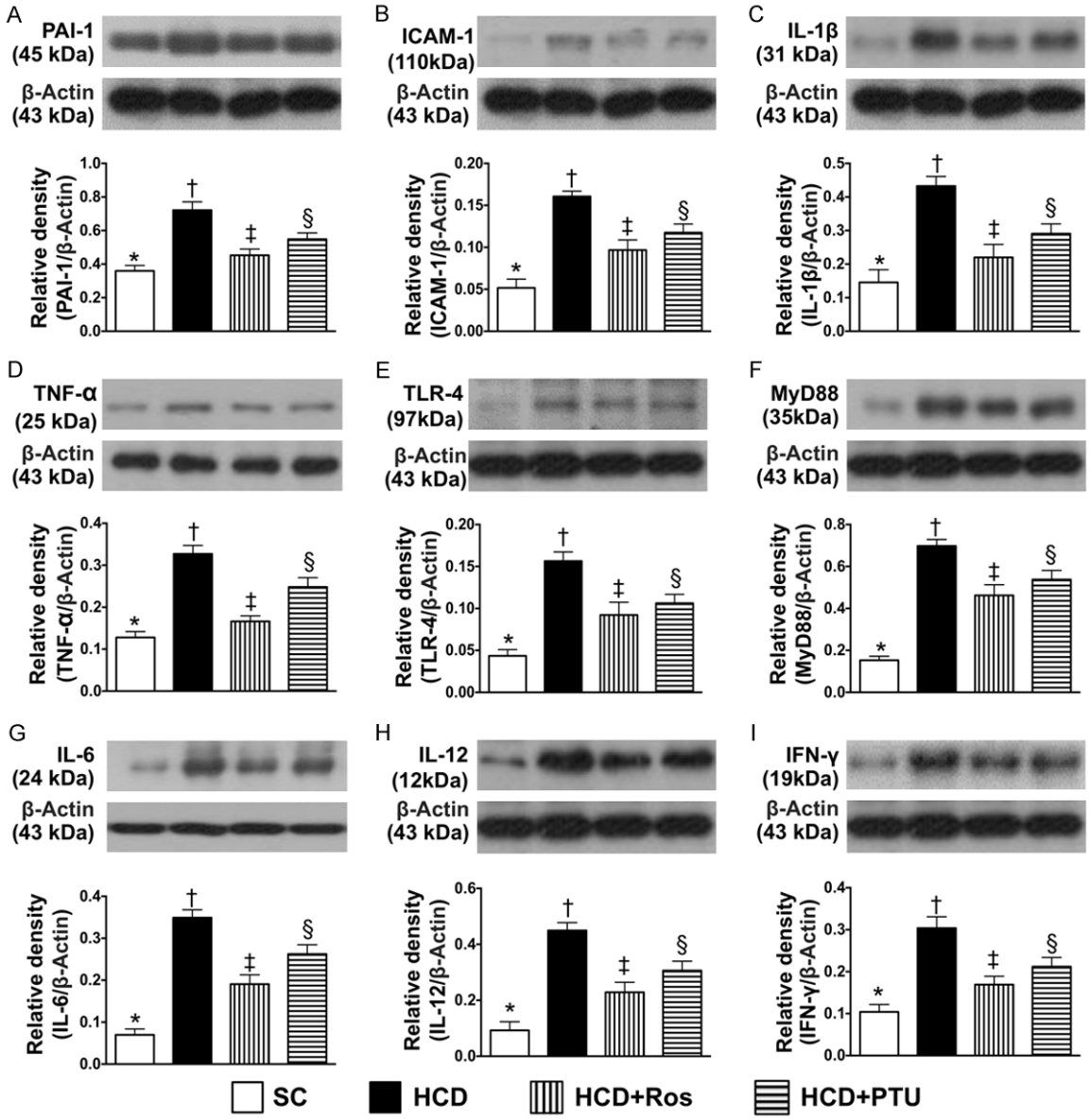

Figure 3. The protein expression of inflammatory biomarkers in liver parenchyma at the 8th week after HCD feeding. A: Protein expression of plasminogen activator inhibitor (PAI)-1, *vs. other groups with different symbols (†, ‡, §), P<0.0001. B: Protein expression of intercellular adhesion molecule (ICAM)-1, *vs. other groups with different symbols (†, ‡, §), P<0.0001. C: Protein expression of interleukin (IL)-1ß, *vs. other groups with different symbols (†, ‡, §), P<0.0001. D: protein expression of tumor necrosis factor (TNF)-α, *vs. other groups with different symbols (†, ‡, §), P<0.0001. E: Protein expression of toll like receptor (TLR)-4, *vs. other groups with different symbols (†, ‡, §), P<0.0001. F: Protein expression of myeloid differentiation factor 88 (MyD88), *vs. other groups with different symbols (†, ‡, §), P<0.0001. G: Protein expression of IL-6, *vs. other groups with different symbols (†, ‡, §), P<0.0001. H: Protein expression of 1L-12, *vs. other groups with different symbols (†, ‡, §), P<0.0001. I: Protein expression interferon gamma (IF-γ), *vs. other groups with different symbols (†, ‡, §), P<0.0001. All statistical analyses were performed by one-way ANOVA, followed by Bonferroni multiple comparison post hoc test (n=8 for each group). Symbols (*, †, ‡, §) indicate significance (at 0.05 level). SC = sham control; HCD = high-cholesterol diet; Ros = rosuvastatin; PTU = propylthiouracil.

The protein expression of cytosolic cytochrome C, an indicator of mitochondrial damage, exhibited an identical pattern to fibrosis among the four groups. On the other hand, the protein expression of mitochondrial cytochrome C, an index of mitochondrial integrity, displayed an opposite pattern to fibrosis among the four groups. Consistently, the protein expressions of SIRT1 and SIRT3, two indicators of oxidative stress suppression, exhibited an identical pat-

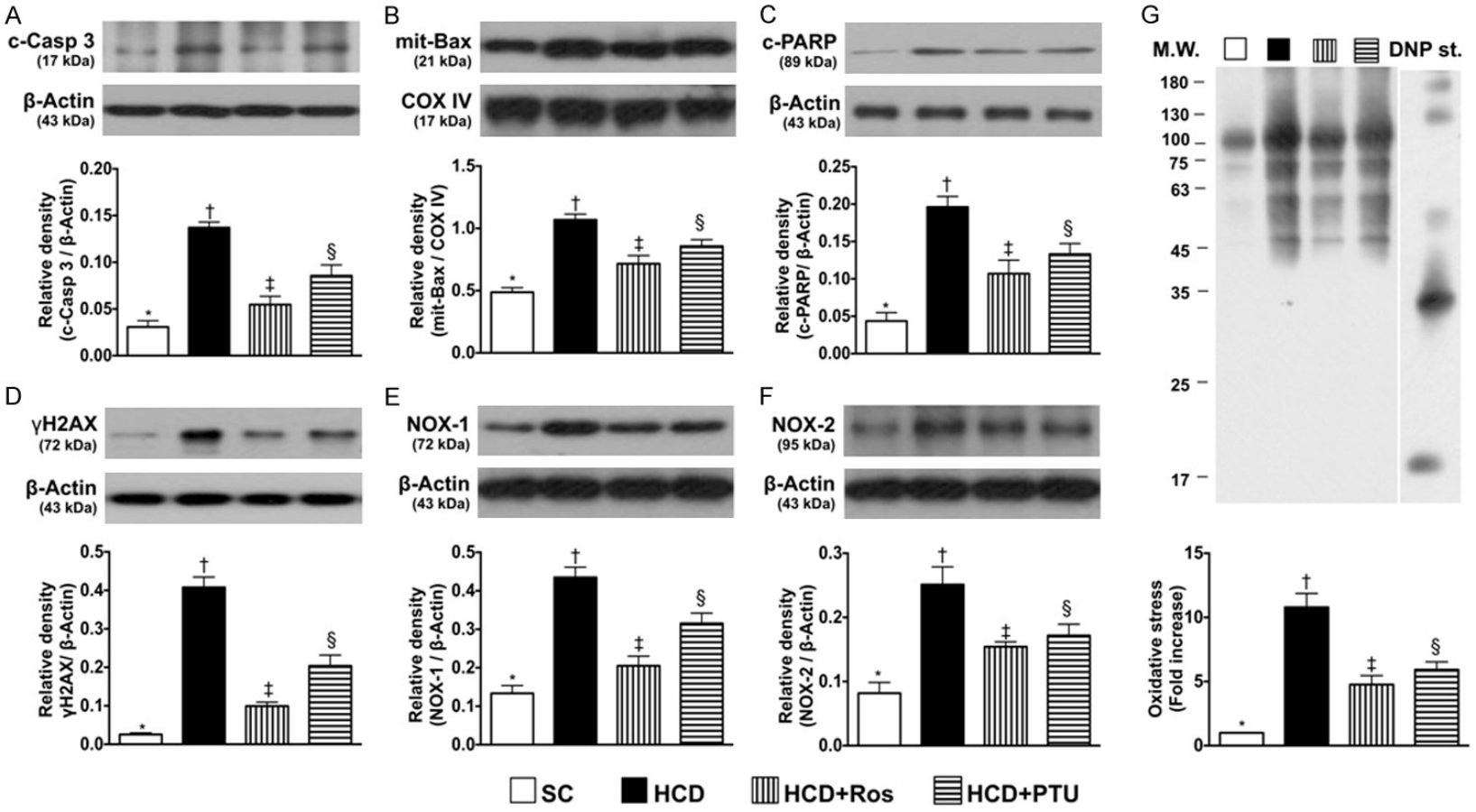

Figure 4. Protein expression of apoptotic, anti-apoptotic, DNA-damaged and oxidative stress biomarkers in liver parenchyma at the 8th week after HCD feeding. A: Protein expression of cleaved caspase 3 (c-Casp 3), *vs. other groups with different symbols (†, ‡, §), P<0.0001. B: Protein expression of mitochondrial Bax, *vs. other groups with different symbols (†, ‡, §), P<0.0001. C: Protein expression of cleaved poly (ADP-ribose) polymerase (c-PARP), *vs. other groups with different symbols (†, ‡, §), P<0.0001. D: Protein expression of γ-H2AX, *vs. other groups with different symbols (†, ‡, §), P<0.0001. E: Protein expression of NOX-1, *vs. other groups with different symbols (†, ‡, §), P<0.0001. F: Protein expression of NOX-2, *vs. other groups with different symbols (†, ‡, §), P<0.0001. G: Protein expression of oxidized protein, *vs. other groups with different symbols (†, ‡, §), P<0.0001. (Note: left and right lanes shown on the upper panel represent protein molecular weight marker and control oxidized molecular protein standard, respectively). M.W = molecular weight; DNP = 1-3 dinitrophenylhydrazone. All statistical analyses were performed by one-way ANOVA, followed by Bonferroni multiple comparison post hoc test (n=8 for each group). Symbols (*, †, ‡, §) indicate significance (at 0.05 level). SC = sham control; HCD = high-cholesterol diet; Ros = rosuvastatin; PTU = propylthiouracil.

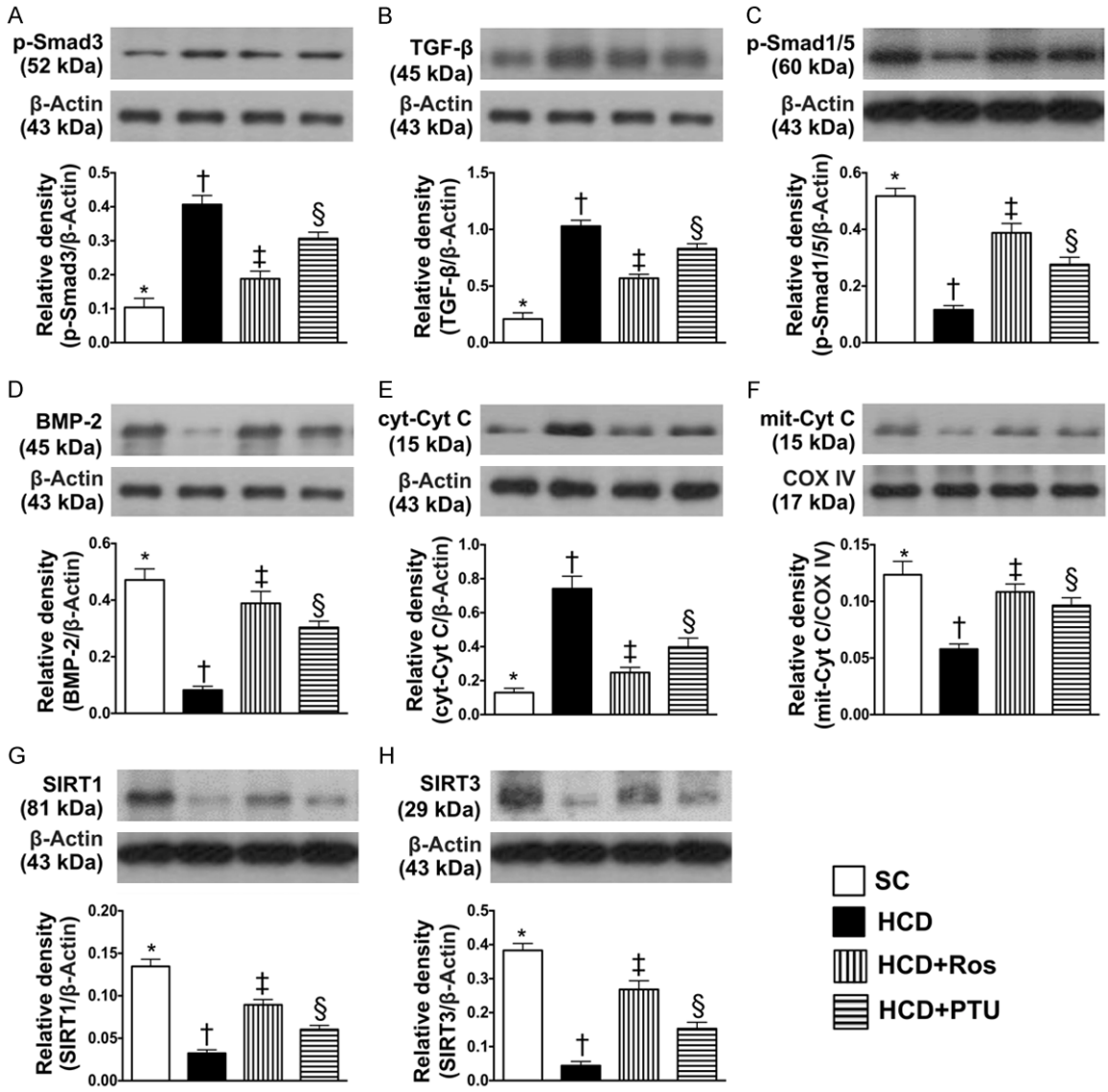

Figure 5. Protein expressions of fibrotic, anti-fibrotic, mitochondrial damaged, mitochondrial-integrity and anti-oxidative stress biomarkers in liver parenchyma at the 8th week after HCD feeding. A: Protein expression of phosphorylated (p)-Smad3, *vs. other groups with different symbols (†, ‡, §), P<0.0001. B: Protein expression of transforming growth factor (TGF)-ß, *vs. other groups with different symbols (†, ‡, §), P<0.0001. C: Protein expression of p-Smad1/5, *vs. other groups with different symbols (†, ‡, §), P<0.0001. D: Protein expression of bone morphogenetic protein (BMP)-2, *vs. other groups with different symbols (†, ‡, §), P<0.0001. E: Protein expression of cytosolic cytochrome C (cyt-Cyto C), *vs. other groups with different symbols (†, ‡, §), P<0.0001. F: Protein expression of mitochondrial cytochrome C (mit-Cyto C), *vs. other groups with different symbols (†, ‡, §), P<0.0001. G: Protein expression of SIRT1, *vs. other groups with different symbols (†, ‡, §), P<0.0001. H: Protein expression of SIRT3, *vs. other groups with different symbols (†, ‡, §), P<0.0001. All statistical analyses were performed by one-way ANOVA, followed by Bonferroni multiple comparison post hoc test (n=8 for each group). Symbols (*, †, ‡, §) indicate significance (at 0.05 level). SC = sham control; HCD = high-cholesterol diet; Ros = rosuvastatin; PTU = propylthiouracil.

tern to mitochondrial cytochrome C among the four groups.

*Inflammatory cellular expressions at the 8th week after HCD feeding (**Figure 6**)*

The IF microscopy showed that the expressions of CD14+ and CD44+ cells, two further indices of inflammation, were highest in group 2, lowest in group 1, and significantly higher in group 4 than in group 3.

*The liver inflammatory and damage biomarkers at the 8th week after HCD feeding (**Figure 7**)*

The IHC microscopy showed that the expressions of Kupffer+ cells, an indicator of inflam-

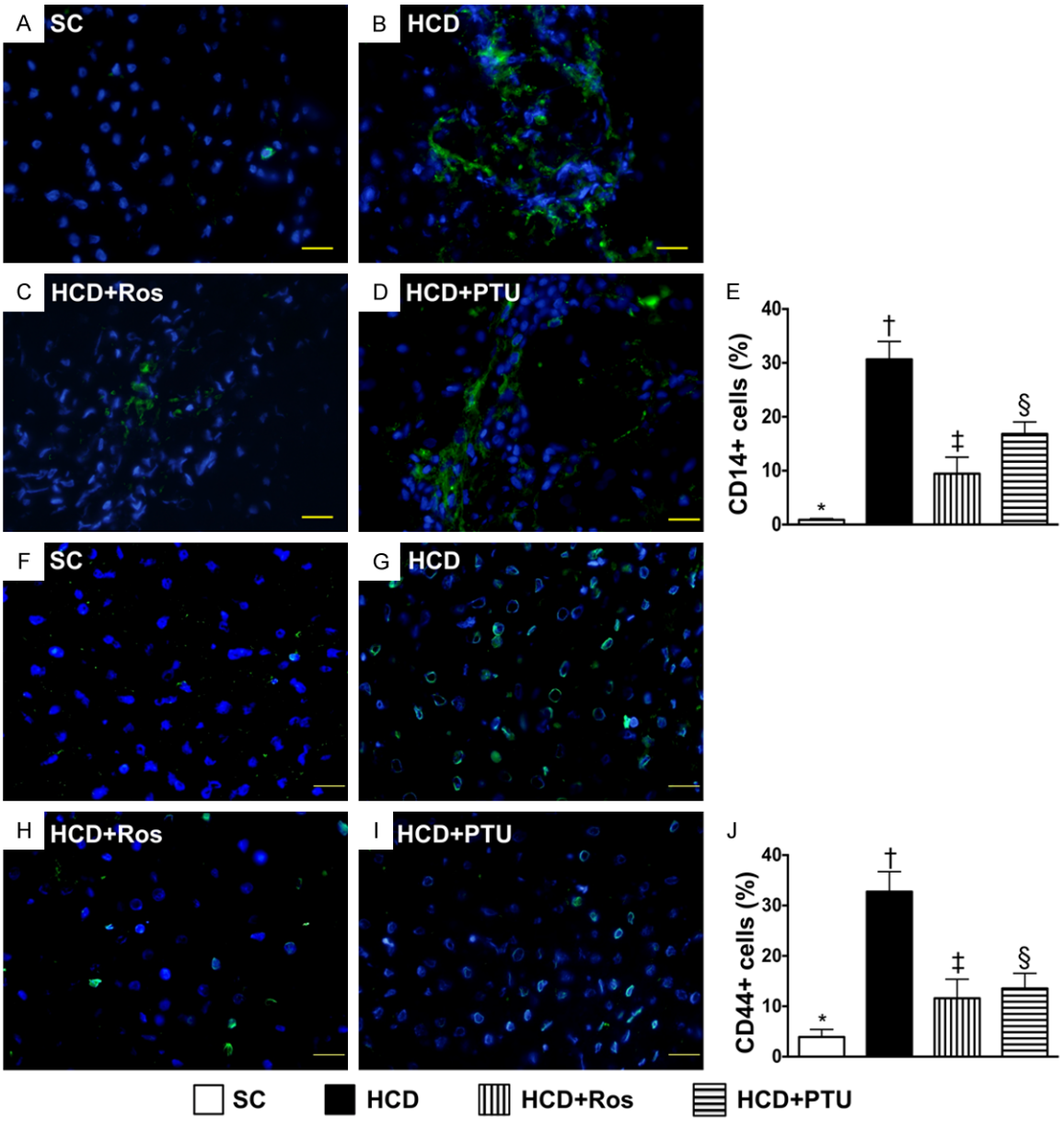

Figure 6. Inflammatory cellular expressions in liver parenchyma at the 8th week after HCD feeding. A-D: Illustrating microscopic finding (400×) of immunofluorescent (IF) staining for identification of CD14+ cells (green). E: Analytical results of number of positively-stained CD14 cells, *vs. other groups with different symbols (†, ‡, §), P<0.0001. F-I: Illustrating microscopic finding (400×) of IF staining for identification of CD44+ cells (green). J: Analytical results of number of positively-stained CD44 cells, *vs. other groups with different symbols (†, ‡, §), P<0.0001. Scale bars in right lower corner represent 20 μm. All statistical analyses were performed by one-way ANOVA, followed by Bonferroni multiple comparison post hoc test (n=8 for each group). Symbols (*, †, ‡, §) indicate significance (at 0.05 level). SC = sham control; HCD = high-cholesterol diet; Ros = rosuvastatin; PTU = propylthiouracil.

mation, were highest in group 2, lowest in group 1, and significantly higher in group 4 than in group 3. Additionally, IHC stain exhibited that the number of α-fetoprotein positively-stained cells displayed an identical pattern to Kupffer cells among the four groups, suggesting that synthesis of α-fetoprotein in hepatocytes implicated a situation of intrinsic response to liver damage. Furthermore, serum levels of AST and ALT, two indices of liver function, also exhibited an identical pattern of Kupffer cells among the four groups.

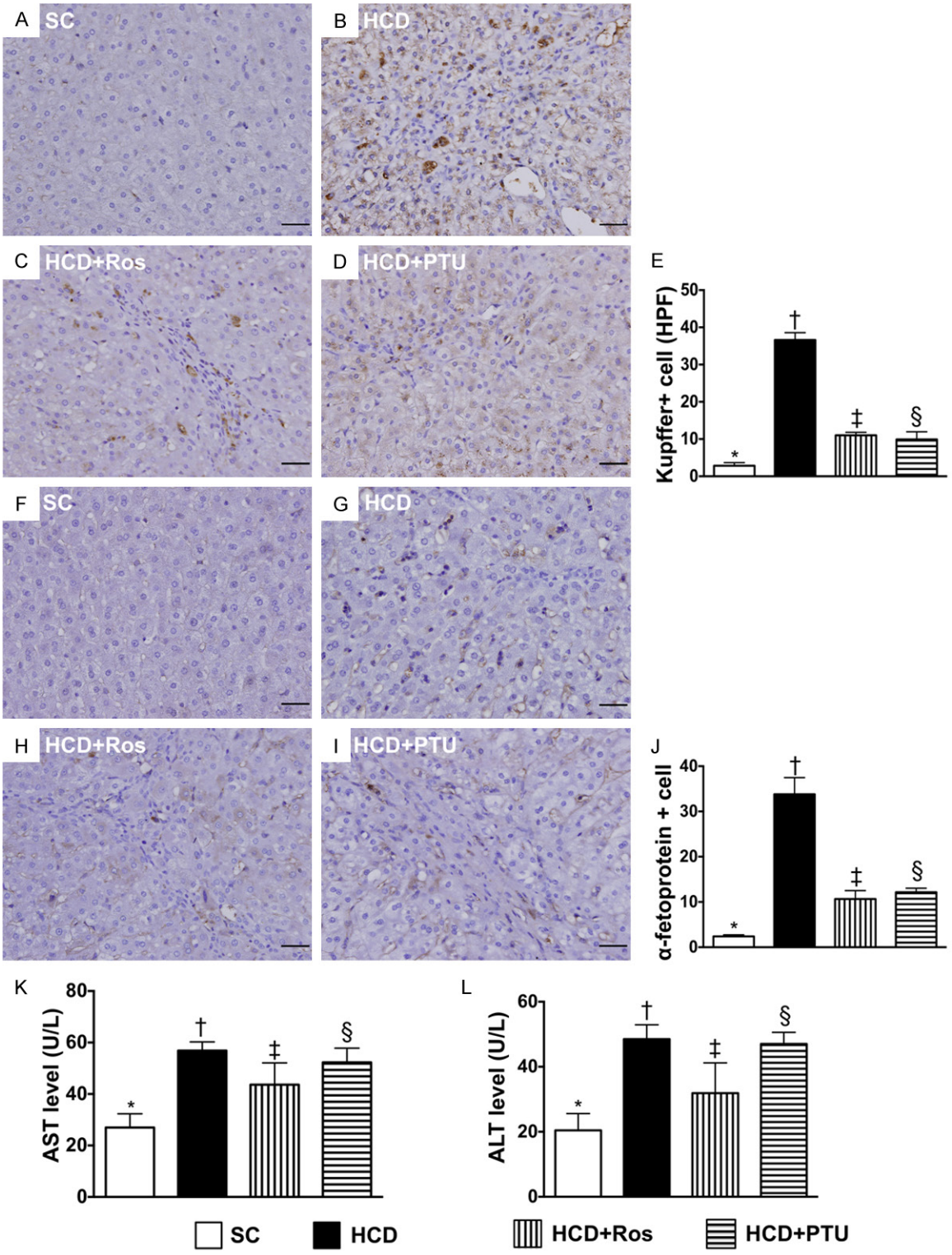

Figure 7. Liver inflammatory and damage biomarkers at the 8th week after HCD feeding. A-D: Illustrating microscopic finding (200×) of immunohistochemical (IHC) staining for identification of Kupffer+ cells (gray). E: Analytical results of number of positively-stained Kupffer cells, *vs. other groups with different symbols (†, ‡, §), P<0.0001. F-I: Illustrating microscopic finding (200×) of IHC staining for identification of α-fetoprotein+ cells (gray). J: Analytical results of number of positively-stained α-fetoprotein cells, *vs. other groups with different symbols (†, ‡, §), P<0.0001. Scale bars in right lower corner represent 50 μm. K: Serum level of aspartate transaminase (AST), *vs. other groups with different symbols (†, ‡, §), P<0.0001. L: Serum level of alanine transaminase (ALT), *vs. other groups with

different symbols (†, ‡, §), P<0.0001. All statistical analyses were performed by one-way ANOVA, followed by Bonferroni multiple comparison post hoc test (n=8 for each group). Symbols (*, †, ‡, §) indicate significance (at 0.05 level). SC = sham control; HCD = high-cholesterol diet; Ros = rosuvastatin; PTU = propylthiouracil.

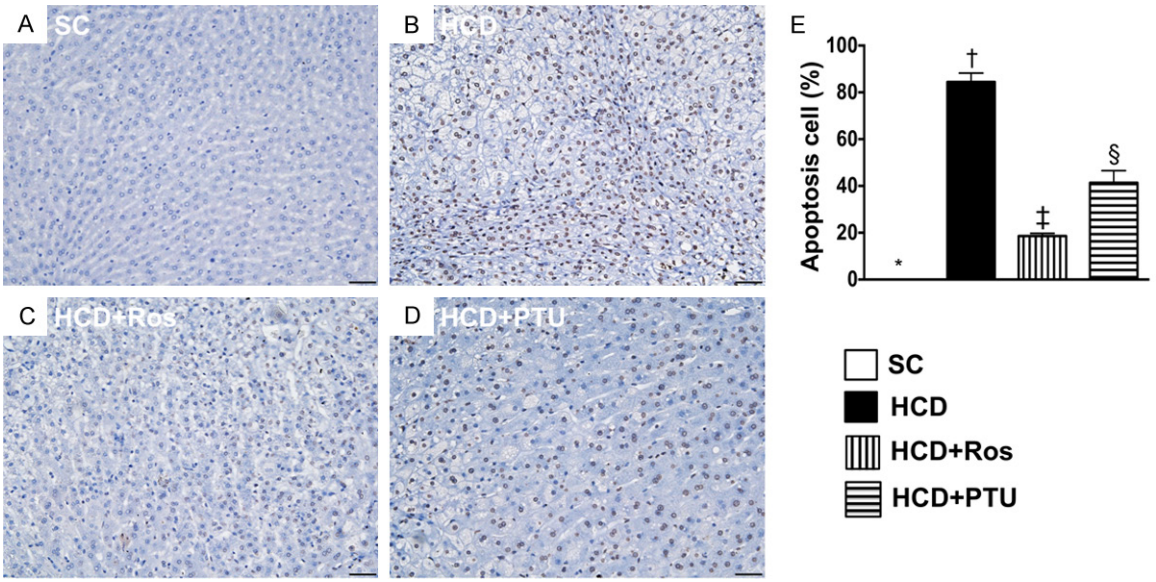

Figure 8. Microscopy for DNA-damaged marker and apoptotic nuclei at the 8th week after HCD feeding. A-D: Illustrating microscopic finding (200×) of TUNEL assay for identification of apoptotic nuclei (gray). E: Analytical results of number of apoptotic nuclei, *vs. other groups with different symbols (†, ‡, §), P<0.0001. Scale bars in right lower corner represent 50 μm. All statistical analyses were performed by one-way ANOVA, followed by Bonferroni multiple comparison post hoc test (n=8 for each group). Symbols (*, †, ‡, §) indicate significance (at 0.05 level). SC = sham control; HCD = high-cholesterol diet; Ros = rosuvastatin; PTU = propylthiouracil.

*Microscopy for apoptotic nuclei at the 8th week after HCD feeding (**Figure 8**)*

IHC microscopy demonstrated that the cellular expression of apoptotic nuclei (i.e., by TUNEL assay) an indicator of DNA-damage, was highest in group 2, lowest in group 1, and significantly higher in group 4 than group 3.

Discussion

This study investigated the impact of HCD on inducing NAFLD in an experimental model and provided several striking implications. First, an experimental model of NAFLD was successfully created by HCD, providing a platform to survey the underlying mechanism of NAFLD. Second, inflammation and the generation of oxidative stress were found to be the main factors involved in the development of NAFLD. Third, Ros-PTU therapy effectively suppressed HCD-induced NAFLD, highlighting that this regimen may have therapeutic potential in clinical setting for NAFLD patients.

Previous studies [17, 31, 32] have shown that NAFLD reflects a process of chronic inflammatory disease and can thus present as a range of severity between simple steatosis to NASH [1-12]. An important finding in the present study was that H&E staining, which identifies lipid accumulation (i.e., inflamed fatty liver implicated steatohepatitis) showed that fat cell distribution was much higher in HCD animals compared to control diet animals. The degree of inflammation according to cellular and protein levels was also substantially increased in HCD animals compared to control diet animals. Accordingly, HCD-induced lipid accumulation plays a crucial role in the initiation and propagation of inflammation in this setting. Furthermore, histopathology showed that the specialized macrophage infiltrations (i.e. Kupffer+ cells in liver parenchyma/walls of sinusoids) in liver verified that inflammation had occurred in HCD animals. Therefore, our findings corroborate the findings of previous studies [17, 31, 32].

Another important finding was that the mitochondrial and DNA damage markers were markedly increased in the HCD group compared to the control diet group. Furthermore, fibrotic (i.e. Masson's trichrome stain) and collagen-deposi-

tion (Sirius red stain) areas, as well as the protein expressions of apoptosis and fibrosis, were remarkably higher in the HCD group than in the control diet group. Additionally, the generation of oxidative stress was significantly higher in HCD animals compared to control diet animals. Interestingly, copious studies have previously identified that inflammation always elicits oxidative stress and vice versa [28, 29, 33]. Thus, these two processes coexist in conditions involving mitochondrial dysfunction, DNA damage, cell apoptosis/death and, ultimately, organ damage [28, 29, 33]. In this way, our findings reinforce those of previous studies [28, 29, 33] and help explain why fibrosis, cell apoptosis and DNA/mitochondrial damage were markedly upregulated in HCD animals compared to control diet animals.

Currently, the treatment of NAFLD/NASH is both uncertain and ineffective [9, 10, 12]. The most important finding in the present study was that inflammation, oxidative stress, apoptosis, mitochondrial/DNA damage and liver fibrosis as well as NAFLD/NASH in HCD animals were all significantly reduced by PTU treatment, and then significantly reduced further by rosuvastatin treatment. Growing clinical [11-13] and experimental [34] studies have shown that statins can improve fatty liver, NAFLD and NASH. The underlying mechanisms of statin treatment in protecting the endothelial cell/vascular wall against atherosclerosis, cells from apoptosis/death and tissue/organs from damage have been established as mainly through suppressing inflammation [18], inhibiting the generation of ROS [19, 20] and reducing the production of oxidant/free radicals [21, 22]. These findings are supported by previous studies [11-13, 18-22, 34] and provide explanation for the improved outcomes observed in HCD animals. However, we have previously shown that PTU can suppress inflammation, oxidative stress, smooth muscle proliferation and arterial atherosclerosis, and enhance nitric oxide (NO) production [25, 26]. In this way, the results of our previous investigations [25, 26] support the findings of our present study, in that PTU treatment suppressed the molecular-cellular perturbations of inflammation, oxidative stress, mitochondrial/DNA damage and liver fibrosis in HCD animals.

Study limitations

Although the findings in the present study are promising, our study has limitations. First, without a HCD group treated by rosuvastatin plus PTU, we were unable to investigate any potential synergistic effect of combining rosuvastatin and PTU for HCD animals. Second, this study only provided tissue and serum (such as aspartate transaminase and alanine transaminase) levels of liver damage biomarkers without imaging investigations by abdominal ultrasound or magnetic resonance imaging (MRI) for evaluating the degree of liver parenchymal disease in living animals.

In conclusion, the present study demonstrated that HCD induced NAFLD/NASH and liver fibrosis in rabbits, and found a therapeutic role for PTU and rosuvastatin for protecting the liver from HCD-induced damage. Rosuvastatin-PTU may therefore be an alternative management strategy for NAFLD, which is a rapidly emerging worldwide health problem.

Acknowledgements

This study was supported by a program grant from Chang Gung Memorial Hospital, Chang Gung University (Grant number: CMRPG8C0751 & CMRPG8C0752).

Disclosure of conflict of interest

None.

Address correspondence to: Dr. Hon-Kan Yip, Division of Cardiology, Department of Internal Medicine, Kaohsiung Chang Gung Memorial Hospital, 123, Dapi Road, Niaosung Dist., Kaohsiung 83301, Taiwan. Tel: +886-7-7317123; Fax: +886-7-73224-02; E-mail: han.gung@msa.hinet.net

References

[1] Chatrath H, Vuppalanchi R and Chalasani N. Dyslipidemia in patients with nonalcoholic fatty liver disease. Semin Liver Dis 2012; 32: 22-29.

[2] Masarone M, Federico A, Abenavoli L, Loguercio C and Persico M. Non alcoholic fatty liver: epidemiology and natural history. Rev Recent Clin Trials 2014; 9: 126-133.

[3] Marchesini G, Brizi M, Bianchi G, Tomassetti S, Bugianesi E, Lenzi M, McCullough AJ, Natale S, Forlani G and Melchionda N. Nonalcoholic fatty liver disease: a feature of the metabolic syndrome. Diabetes 2001; 50: 1844-1850.

[4] Hsiao PJ, Kuo KK, Shin SJ, Yang YH, Lin WY, Yang JF, Chiu CC, Chuang WL, Tsai TR and Yu ML. Significant correlations between severe fatty liver and risk factors for metabolic syn-

drome. J Gastroenterol Hepatol 2007; 22: 2118-2123.
[5] Angulo P. Nonalcoholic fatty liver disease. N Engl J Med 2002; 346: 1221-1231.
[6] Chalasani N, Younossi Z, Lavine JE, Diehl AM, Brunt EM, Cusi K, Charlton M and Sanyal AJ. The diagnosis and management of non-alcoholic fatty liver disease: practice guideline by the American association for the study of liver diseases, American college of gastroenterology, and the American gastroenterological association. Hepatology 2012; 55: 2005-2023.
[7] Nascimbeni F, Pais R, Bellentani S, Day CP, Ratziu V, Loria P and Lonardo A. From NAFLD in clinical practice to answers from guidelines. J Hepatol 2013; 59: 859-871.
[8] Younossi ZM, Stepanova M, Afendy M, Fang Y, Younossi Y, Mir H and Srishord M. Changes in the prevalence of the most common causes of chronic liver diseases in the United States from 1988 to 2008. Clin Gastroenterol Hepatol 2011; 9: 524-530, e521; quiz e560.
[9] Milic S, Lulic D and Stimac D. Non-alcoholic fatty liver disease and obesity: biochemical, metabolic and clinical presentations. World J Gastroenterol 2014; 20: 9330-9337.
[10] Younossi ZM, Stepanova M, Henry L, Racila A, Lam B, Pham HT and Hunt S. A disease-specific quality of life instrument for non-alcoholic fatty liver disease and non-alcoholic steatohepatitis: CLDQ-NAFLD. Liver Int 2017; 37: 1209-1218.
[11] Sayiner M, Koenig A, Henry L and Younossi ZM. Epidemiology of nonalcoholic fatty liver disease and nonalcoholic steatohepatitis in the United States and the rest of the world. Clin Liver Dis 2016; 20: 205-214.
[12] Eslami L, Merat S, Malekzadeh R, Nasseri-Moghaddam S and Aramin H. Statins for non-alcoholic fatty liver disease and non-alcoholic steatohepatitis. Cochrane Database Syst Rev 2013; CD008623.
[13] Tziomalos K, Athyros VG, Paschos P and Karagiannis A. Nonalcoholic fatty liver disease and statins. Metabolism 2015; 64: 1215-1223.
[14] Yopp AC and Choti MA. Non-alcoholic steatohepatitis-related hepatocellular carcinoma: a growing epidemic? Dig Dis 2015; 33: 642-647.
[15] Pocha C, Kolly P and Dufour JF. Nonalcoholic fatty liver disease-related hepatocellular carcinoma: a problem of growing magnitude. Semin Liver Dis 2015; 35: 304-317.
[16] Perumpail RB, Wong RJ, Ahmed A and Harrison SA. Hepatocellular carcinoma in the setting of non-cirrhotic nonalcoholic fatty liver disease and the metabolic syndrome: US experience. Dig Dis Sci 2015; 60: 3142-3148.
[17] Streba LA, Vere CC, Rogoveanu I and Streba CT. Nonalcoholic fatty liver disease, metabolic risk factors, and hepatocellular carcinoma: an open question. World J Gastroenterol 2015; 21: 4103-4110.
[18] Ridker PM, Danielson E, Fonseca FA, Genest J, Gotto AM Jr, Kastelein JJ, Koenig W, Libby P, Lorenzatti AJ, MacFadyen JG, Nordestgaard BG, Shepherd J, Willerson JT, Glynn RJ; JUPITER Study Group. Rosuvastatin to prevent vascular events in men and women with elevated C-reactive protein. N Engl J Med 2008; 359: 2195-2207.
[19] Chartoumpekis D, Ziros PG, Psyrogiannis A, Kyriazopoulou V, Papavassiliou AG and Habeos IG. Simvastatin lowers reactive oxygen species level by Nrf2 activation via PI3K/Akt pathway. Biochem Biophys Res Commun 2010; 396: 463-466.
[20] Li J, Wang JJ, Yu Q, Chen K, Mahadev K and Zhang SX. Inhibition of reactive oxygen species by Lovastatin downregulates vascular endothelial growth factor expression and ameliorates blood-retinal barrier breakdown in db/db mice: role of NADPH oxidase 4. Diabetes 2010; 59: 1528-1538.
[21] Parizadeh SM, Azarpazhooh MR, Moohebati M, Nematy M, Ghayour-Mobarhan M, Tavallaie S, Rahsepar AA, Amini M, Sahebkar A, Mohammadi M and Ferns GA. Simvastatin therapy reduces prooxidant-antioxidant balance: results of a placebo-controlled cross-over trial. Lipids 2011; 46: 333-340.
[22] Dummer CD, Thome FS, Zingano B, Lindoso A and Veronese FV. Acute effect of simvastatin on inflammation and oxidative stress in chronic kidney disease. J Nephrol 2008; 21: 900-908.
[23] Nicholls SJ, Ballantyne CM, Barter PJ, Chapman MJ, Erbel RM, Libby P, Raichlen JS, Uno K, Borgman M, Wolski K and Nissen SE. Effect of two intensive statin regimens on progression of coronary disease. N Engl J Med 2011; 365: 2078-2087.
[24] Lin YC, Chiang CH, Chang LT, Sun CK, Leu S, Shao PL, Hsieh MC, Tsai TH, Chua S, Chung SY, Kao YH and Yip HK. Simvastatin attenuates the additive effects of TNF-alpha and IL-18 on the connexin 43 up-regulation and over-proliferation of cultured aortic smooth muscle cells. Cytokine 2013; 62: 341-351.
[25] Sun CK, Yuen CM, Kao YH, Chang LT, Chua S, Sheu JJ, Yen CH, Ko SF and Yip HK. Propylthiouracil attenuates monocrotaline-induced pulmonary arterial hypertension in rats. Circ J 2009; 73: 1722-1730.
[26] Lin PY, Lee FY, Wallace CG, Chen KH, Kao GS, Sung PH, Chua S, Ko SF, Chen YL, Wu SC, Chang HW, Yip HK and Shao PL. The therapeutic effect of rosuvastatin and propylthiouracil on ameliorating high-cholesterol diet-induced rabbit aortic atherosclerosis and stiffness. Int J Cardiol 2017; 227: 938-949.

[27] Yen CH, Sun CK, Leu S, Wallace CG, Lin YC, Chang LT, Chen YL, Tsa TH, Kao YH, Shao PL, Hsieh CY, Chen YT and Yip HK. Continuing exposure to low-dose nonylphenol aggravates adenine-induced chronic renal dysfunction and role of rosuvastatin therapy. J Transl Med 2012; 10: 147.

[28] Chua S, Lee FY, Chiang HJ, Chen KH, Lu HI, Chen YT, Yang CC, Lin KC, Chen YL, Kao GS, Chen CH, Chang HW and Yip HK. The cardioprotective effect of melatonin and exendin-4 treatment in a rat model of cardiorenal syndrome. J Pineal Res 2016; 61: 438-456.

[29] Chen KH, Chen CH, Wallace CG, Yuen CM, Kao GS, Chen YL, Shao PL, Chen YL, Chai HT, Lin KC, Liu CF, Chang HW, Lee MS and Yip HK. Intravenous administration of xenogenic adipose-derived mesenchymal stem cells (ADMSC) and ADMSC-derived exosomes markedly reduced brain infarct volume and preserved neurological function in rat after acute ischemic stroke. Oncotarget 2016; 7: 74537-74556.

[30] Huang TH, Chung SY, Chua S, Chai HT, Sheu JJ, Chen YL, Chen CH, Chang HW, Tong MS, Sung PH, Sun CK, Lu HI and Yip HK. Effect of early administration of lower dose versus high dose of fresh mitochondria on reducing monocrotaline-induced pulmonary artery hypertension in rat. Am J Transl Res 2016; 8: 5151-5168.

[31] Lou Y, Chen YD, Sun FR, Shi JP, Song Y and Yang J. Potential regulators driving the transition in nonalcoholic fatty liver disease: a stage-based view. Cell Physiol Biochem 2017; 41: 239-251.

[32] du Plessis J, van Pelt J, Korf H, Mathieu C, van der Schueren B, Lannoo M, Oyen T, Topal B, Fetter G, Nayler S, van der Merwe T, Windmolders P, Van Gaal L, Verrijken A, Hubens G, Gericke M, Cassiman D, Francque S, Nevens F and van der Merwe S. Association of adipose tissue inflammation with histologic severity of nonalcoholic fatty liver disease. Gastroenterology 2015; 149: 635-648, e614.

[33] Day YJ, Chen KH, Chen YL, Huang TH, Sung PH, Lee FY, Chen CH, Chai HT, Yin TC, Chiang HJ, Chung SY, Chang HW and Yip HK. Preactivated and disaggregated shape-changed platelets protected against acute respiratory distress syndrome complicated by sepsis through inflammation suppression. Shock 2016; 46: 575-586.

[34] Park HS, Jang JE, Ko MS, Woo SH, Kim BJ, Kim HS, Park HS, Park IS, Koh EH and Lee KU. Statins increase mitochondrial and peroxisomal fatty acid oxidation in the liver and prevent non-alcoholic steatohepatitis in mice. Diabetes Metab J 2016; 40: 376-385.